



0142964

1
NACA RM A50K27a~~CONFIDENTIAL~~

NATIONAL ADVISORY COMMITTEE FOR AERONAUTICS

RESEARCH MEMORANDUMLIFT, DRAG, AND PITCHING MOMENT OF LOW-ASPECT-RATIO WINGS
AT SUBSONIC AND SUPERSONIC SPEEDS - TRIANGULAR WING
OF ASPECT RATIO 2 WITH NACA 0005-63 THICKNESS
DISTRIBUTION, CAMBERED AND TWISTED FOR A
TRAPEZOIDAL SPAN LOAD DISTRIBUTION

By Willard G. Smith and E. Ray Phelps

SUMMARY

A wing-body combination having a plane triangular wing of aspect ratio 2 with NACA 0005-63 thickness distribution in streamwise planes, and twisted and cambered for a trapezoidal span load distribution has been investigated at both subsonic and supersonic Mach numbers. The lift, drag, and pitching moment of the model are presented for Mach numbers from 0.60 to 0.90 and 1.30 to 1.70 at a Reynolds number of 3.0 million. The variations of the characteristics with Reynolds number are also shown for several Mach numbers.

INTRODUCTION

A research program is in progress at the Ames Aeronautical Laboratory to ascertain experimentally at subsonic and supersonic Mach numbers the characteristics of wings of interest in the design of high-speed fighter airplanes. Variations in plan form, twist, camber, and thickness are being investigated. This report is one of a series pertaining to this program and presents results of tests of a wing-body combination having a triangular wing of aspect ratio 2 with NACA 0005-63 thickness distribution in streamwise planes, and twisted and cambered for a trapezoidal span load distribution. Results of other investigations in this program are presented in references 1 to 5. As in these references, the data herein are presented without analysis to expedite publication.

NOTATION

b wing span, feet

~~CONFIDENTIAL~~

37-148-56

- \bar{c} mean aerodynamic chord $\left(\frac{\int_0^{b/2} c^2 dy}{\int_0^{b/2} c dy} \right)$, feet
- c projected local wing chord, feet
- l length of body including portion removed to accommodate sting, inches
- $\frac{L}{D}$ lift-drag ratio
- $\left(\frac{L}{D} \right)_{\max}$ maximum lift-drag ratio
- M Mach number
- q free-stream dynamic pressure, pounds per square foot
- R Reynolds number based on the mean aerodynamic chord
- r radius of body, inches
- r_0 maximum body radius, inches
- S total projected wing area, including area formed by extending leading and trailing edges to plane of symmetry, square feet
- X distance from wing leading edge in wing reference plane, inches
- x longitudinal distance from nose of body, inches
- Z vertical distance from wing reference plane, inches
- y distance perpendicular to plane of symmetry, feet
- α angle of attack of body axis, degrees
- C_D drag coefficient $\left(\frac{\text{drag}}{qS} \right)$
- C_L lift coefficient $\left(\frac{\text{lift}}{qS} \right)$
- C_m pitching-moment coefficient referred to quarter point of mean aerodynamic chord $\left(\frac{\text{pitching moment}}{qS\bar{c}} \right)$

$\frac{dC_L}{d\alpha}$ slope of the lift curve measured at zero lift, per degree

$\frac{dC_m}{dC_L}$ slope of the pitching-moment curve measured at zero lift

Subscripts

U upper surface of wing

L lower surface of wing

APPARATUS

Wind Tunnel and Equipment

The experimental investigation was conducted in the Ames 6- by 6-foot supersonic wind tunnel. In this wind tunnel, the Mach number can be varied continuously and the stagnation pressure can be regulated to maintain a given test Reynolds number. The air is dried to prevent formation of condensation shocks. Further information on this wind tunnel is presented in reference 6.

The model was sting mounted in the tunnel, the diameter of the sting being about 73 percent of the diameter of the body base. The pitch plane of the model support was horizontal in the wind tunnel. A balance mounted on the sting support and enclosed within the body of the model was used to measure the aerodynamic forces and moments on the model. The balance was the 4-inch, four-component strain-gage balance described in reference 7.

Model

A photograph of the model mounted in the Ames 6- by 6-foot wind tunnel is shown in figure 1. A plan view of the model and certain model dimensions are given in figure 2. Other important geometric characteristics of the model are as follows:

Wing

Aspect ratio	2
Taper ratio	0
Thickness distribution (streamwise).	NACA 0005-63
Total area, S, square feet	4.014
Mean aerodynamic chord, \bar{c} , feet.	1.889
Incidence, degrees	0
Distance, wing reference plane to body axis, feet	0

Body

Fineness ratio (based on length, l ; fig. 2).12.5
Cross-section shape	Circular
Maximum cross-sectional area, square feet	0.204
Ratio of maximum cross-sectional area to wing area	0.0509

The twist and camber of the present wing was derived from a theoretical equation satisfying the linearized supersonic potential flow equation and giving the shape of a surface for a uniform pressure distribution. (See reference 8.) At the design Mach number of 1.53 and design lift coefficient of 0.25 the span load distribution was trapezoidal, being constant to 62.5 percent of the semispan and varying linearly from there to zero at the tip. The section coordinates for this wing are given in table I.

The wing was constructed of solid steel. The body spar was also steel and covered with aluminum to form the body contours. The surfaces of the wing and body were polished smooth.

TESTS AND PROCEDURE

Range of Test Variables

The characteristics of the model (as a function of angle of attack) were investigated for a range of Mach numbers from 0.60 to 0.90 and from 1.30 to 1.70. The major portion of the data was obtained at a Reynolds number of 3.0 million. Data were also obtained for Reynolds number up to 7.5 million at Mach numbers of 0.80, 1.40, and 1.60.

Reduction of Data

The test data have been reduced to standard NACA coefficient form. Factors which could affect the accuracy of these results and the corrections applied are discussed in the following paragraphs.

Tunnel-wall interference.— Corrections to the subsonic results for the induced effects of the tunnel walls resulting from lift on the model were made according to the methods of reference 9. The numerical values of these corrections (which were added to the uncorrected data) were

$$\Delta\alpha = 0.93 C_L$$

$$\Delta C_D = 0.016 C_L^2$$

No corrections were made to the pitching-moment coefficients.

The effects of constriction of the flow at subsonic speeds by the tunnel walls were taken into account by the method of reference 10. This correction was calculated for conditions at zero angle of attack and was applied throughout the angle-of-attack range. At a Mach number of 0.90, this correction amounted to a 4-percent increase in the Mach number over that determined from a calibration of the wind tunnel without a model in place.

For the tests at supersonic speeds, the reflection from the tunnel walls of the Mach wave originating at the nose of the body did not cross the model. No corrections were required, therefore, for tunnel-wall effects.

Stream variations.— Tests at subsonic speeds in the 6- by 6-foot supersonic wind tunnel of a symmetrical model in both the normal and the inverted positions have indicated no stream curvature or inclination in the pitch plane of the model. No measurements have been made, however, of the stream curvature in the yaw plane. At subsonic speeds, the longitudinal variation of static pressure in the region of the model is not known accurately at present, but a preliminary survey has indicated that it is less than 2 percent of the dynamic pressure. No correction for this effect was made.

A survey of the air stream in the wind tunnel at supersonic speeds (reference 6) has shown a stream curvature only in the yaw plane of the model. The effects of this curvature on the measured characteristics of the present model are not known, but are believed to be small as judged by the results of reference 11. The survey also indicated that there is a static-pressure variation in the test section of sufficient magnitude to affect the drag results. A correction was added to the measured drag coefficient, therefore, to account for the longitudinal buoyancy caused by this static-pressure variation. This correction varied from as much as -0.0008 at a Mach number of 1.30 to +0.0009 at a Mach number of 1.70.

Support interference.— At subsonic speeds, the effects of support interference on the aerodynamic characteristics of the model are not known. For the present tailless model, it is believed that such effects

consisted primarily of a change in the pressure at the base of the model. In an effort to correct at least partially for this support interference, the base pressure was measured and the drag data were adjusted to correspond to a base pressure equal to the static pressure of the free stream.

At supersonic speeds, the effects of support interference of a body-sting configuration similar to that of the present model are shown by reference 12 to be confined to a change in base pressure. The previously mentioned adjustment of the drag for base pressure, therefore, was applied at supersonic speeds.

RESULTS

The results are presented in this report without analysis in order to expedite publication. Figure 3 shows the variation of lift coefficient with angle of attack and the variation of drag coefficient, pitching-moment coefficient, and lift-drag ratio with lift coefficient at a Reynolds number of 3.0 million and at Mach numbers from 0.60 to 1.70. The effect of Reynolds number on the aerodynamic characteristics at Mach numbers of 0.80, 1.40, and 1.60 is shown in figure 4. The results presented in figure 3 have been summarized in figure 5 to show some important parameters as functions of Mach number. The slope parameters in this figure have been measured at zero lift.

Ames Aeronautical Laboratory,
National Advisory Committee for Aeronautics,
Moffett Field, Calif.

REFERENCES

1. Smith, Donald W., and Heitmeyer, John C.: Lift, Drag, and Pitching-Moment of Low-Aspect-Ratio Wings at Subsonic and Supersonic Speeds - Plane Triangular Wing of Aspect Ratio 2 With NACA 0008-63 Section. NACA RM A50K20, 1950.
2. Smith, Donald W., and Heitmeyer, John C.: Lift, Drag, and Pitching Moment of Low-Aspect-Ratio Wings at Subsonic and Supersonic Speeds - Plane Triangular Wing of Aspect Ratio 2 With NACA 0005-63 Section. NACA RM A50K21, 1950.

3. Heitmeyer, John C., and Stephenson, Jack D.: Lift, Drag, and Pitching Moment of Low-Aspect-Ratio Wings at Subsonic and Supersonic Speeds - Plane Triangular Wing of Aspect Ratio 4 With NACA 0005-63 Section. NACA RM A50K24, 1950.
4. Phelps, E. Ray, and Smith, Willard G.: Lift, Drag, and Pitching Moment of Low-Aspect-Ratio Wings at Subsonic and Supersonic Speeds - Triangular Wing of Aspect Ratio 4 With NACA 0005-63 Thickness Distribution, Cambered and Twisted for Trapezoidal Span Load Distribution. NACA RM A50K24b, 1950.
5. Heitmeyer, John C., and Smith, Willard G.: Lift, Drag, and Pitching Moment of Low-Aspect-Ratio Wings at Subsonic and Supersonic Speeds - Plane Triangular Wing of Aspect Ratio 2 With NACA 0003-63 Section. NACA RM A50K24a, 1950.
6. Frick, Charles W., and Olson, Robert N.: Flow Studies in the Asymmetric Adjustable Nozzle of the Ames 6- by 6-foot Supersonic Wind Tunnel. NACA RM A9E24, 1949.
7. Olson, Robert N., and Mead, Merrill H.: Aerodynamic Study of a Wing-Fuselage Combination Employing a Wing Swept Back 63° - Effectiveness of an Elevon as a Longitudinal Control and the Effects of Camber and Twist on the Maximum Lift-Drag Ratio at Supersonic Speeds. NACA RM A50A31a, 1950.
8. Jones, Robert T.: Estimated Lift-Drag Ratios at Supersonic Speeds. NACA TN 1350, 1947.
9. Glauert, H.: The Elements of Aerofoil and Airscrew Theory. The University Press, Cambridge, England, 1926, ch. XIV.
10. Herriot, John G.: Blockage Corrections for Three-Dimensional-Flow Closed-Throat Wind Tunnels, with Consideration of the Effect of Compressibility. NACA RM A7B28, 1947.
11. Lessing, Henry C.: Aerodynamic Study of a Wing-Fuselage Combination Employing a Wing Swept Back 63° - Effect of Sideslip on Aerodynamic Characteristics at a Mach Number of 1.4 With the Wing Twisted and Cambered. NACA RM A50F09, 1950.
12. Perkins, Edward W.: Experimental Investigation of the Effects of Support Interference on the Drag of Bodies of Revolution at a Mach Number of 1.5. NACA RM A8B05, 1948.

TABLE I

COORDINATES FOR TWISTED AND CAMBERED TRIANGULAR WING OF ASPECT RATIO 2

Station 0 (symmetrical)		Station 2.500				Station 3.400				Station 5.100				Station 6.800			
X	Z	X _U	Z _U	X _L	Z _L	X _U	Z _U	X _L	Z _L	X _U	Z _U	X _L	Z _L	X _U	Z _U	X _L	Z _L
0.000	0.000	0.000	0.409	0.000	0.409	0.000	0.577	0.000	0.577	0.000	0.836	0.000	0.836	0.000	1.114	0.000	1.114
.426	.269	.330	.703	.385	.846	.304	.839	.366	.412	.260	1.050	.325	.718	.218	1.338	.282	1.060
.853	.371	.695	.826	.742	.193	.643	.961	.703	.369	.752	1.208	.622	.691	.466	1.446	.588	1.005
1.706	.505	1.438	.977	1.448	.114	1.332	1.112	1.371	.303	1.147	1.368	1.211	.662	.972	1.525	1.045	.991
2.559	.597	2.158	1.036	2.147	.018	2.068	1.213	2.036	.256	1.747	1.477	1.797	.641	1.482	1.706	1.549	.991
3.411	.665	3.005	1.005	2.808	-.114	2.732	1.299	2.697	.193	2.351	1.554	2.383	.620	1.994	1.750	2.053	.990
5.117	.759	4.415	.921	4.336	-.374	4.196	1.181	3.925	-.018	3.566	1.634	3.554	.567	3.025	1.502	3.060	.988
6.823	.815	5.660	.806	5.811	-.489	5.524	1.057	5.417	-.245	4.797	1.686	4.718	.483	4.059	1.371	4.067	.989
8.283	.844	7.311	.688	7.277	-.553	6.873	1.003	6.810	-.348	6.067	1.448	5.862	.317	5.088	1.169	5.083	.973
10.234	.853	8.764	.566	8.739	-.590	8.233	.927	8.187	-.409	7.225	1.308	7.092	.222	6.145	1.034	6.089	.909
13.646	.825	11.672	.800	11.657	-.607	10.958	.865	10.922	-.437	9.608	1.102	9.547	-.054	8.269	1.051	8.097	.673
17.057	.752	14.581	.717	14.571	-.567	13.686	.761	13.670	-.444	11.993	.942	11.975	-.206	10.302	1.324	10.805	.423
20.468	.650	17.490	.610	17.484	-.497	16.415	.647	16.405	-.392	14.383	.765	14.356	-.205	12.337	1.115	12.831	.335
23.880	.520	20.402	.483	20.397	-.406	19.145	.518	19.138	-.316	16.767	.662	16.753	-.068	14.381	.938	14.355	.311
27.291	.373	23.311	.341	23.309	-.295	21.874	.380	21.870	-.217	19.156	.516	19.148	-.006	16.429	.772	16.414	.323
30.703	.205	26.221	.188	26.220	-.162	24.603	.230	24.600	-.099	21.544	.365	21.541	.076	18.477	.610	18.470	.363
32.408	.114	27.676	.107	27.675	-.088	25.968	.148	25.967	-.035	22.739	.286	22.737	.125	19.700	.537	19.456	.399
34.114	.017	29.131	.020	29.131	-.010	27.333	.067	27.333	.038	23.933	.205	23.933	.180	20.524	.447	20.524	.426
Leading-edge radius: 0.113		Leading-edge radius: 0.097				Leading-edge radius: 0.091				Leading-edge radius: 0.079				Leading-edge radius: 0.068			

Station 8.700				Station 10.200				Station 11.900				Station 13.600				Station 15.300			
X _U	Z _U	X _L	Z _L	X _U	Z _U	X _L	Z _L	X _U	Z _U	X _L	Z _L	X _U	Z _U	X _L	Z _L	X _U	Z _U	X _L	Z _L
0.000	1.393	0.000	1.393	0.000	1.672	0.000	1.672	0.000	1.950	0.000	1.950	0.000	2.229	0.000	2.229	0.000	2.508	0.000	0.000
.178	1.528	.238	1.320	.140	1.827	.192	1.617	.103	2.069	.145	1.913	.066	2.310	.099	2.207	.030	2.549	.051	2.500
.354	1.677	.432	1.311	.303	1.906	.364	1.615	.224	2.131	.275	1.914	.147	2.354	.185	2.210	.088	2.573	.094	2.503
.742	1.816	.875	1.312	.636	2.023	.703	1.624	.472	2.224	.530	1.928	.310	2.422	.377	2.225	.132	2.611	.179	2.513
1.227	1.916	1.296	1.321	.972	2.112	1.041	1.639	.723	2.298	.785	1.946	.477	2.475	.324	2.242	.235	2.640	.263	2.525
1.649	1.977	1.716	1.313	1.310	2.126	1.377	1.657	.975	2.360	1.036	1.966	.644	2.523	.493	2.261	.318	2.669	.348	2.539
2.502	2.118	2.554	1.357	1.989	2.301	2.050	1.696	1.422	2.460	1.541	2.009	.921	2.599	1.025	2.300	.489	2.715	.516	2.566
3.359	2.197	3.398	1.379	2.670	2.325	2.723	1.734	1.991	2.538	2.043	2.093	1.318	2.663	1.365	2.341	.673	2.755	.624	2.594
4.218	2.240	4.241	1.393	3.354	2.446	3.396	1.771	2.501	2.599	2.520	2.096	1.697	2.715	1.702	2.381	.821	2.787	.851	2.621
5.077	2.263	5.084	1.407	4.032	2.487	4.071	1.825	3.012	2.628	3.093	2.139	1.997	2.759	2.037	2.421	1.020	2.819	1.012	2.651
6.201	2.228	6.774	1.401	5.402	2.523	5.422	1.863	4.026	2.713	4.066	2.220	2.276	2.828	2.709	2.501	1.320	2.871	1.353	2.708
6.737	2.086	8.467	1.334	6.720	2.502	6.777	1.902	5.021	2.744	5.080	2.294	3.257	2.820	3.261	2.522	1.668	2.912	1.629	2.763
10.226	1.773	10.173	1.132	8.154	2.437	8.137	1.918	6.026	2.747	6.095	2.359	4.039	2.910	4.027	2.672	2.007	2.947	2.024	2.818
11.922	1.453	11.920	.993	9.590	2.319	9.501	1.903	7.111	2.725	7.114	2.414	4.720	2.929	4.733	2.722	2.347	2.976	2.359	2.873
13.622	1.202	13.661	.829	10.910	2.120	10.873	1.824	8.137	2.621	8.135	2.457	5.402	2.936	5.409	2.722	2.637	2.999	2.699	2.925
15.327	1.009	15.325	.802	12.229	1.824	12.221	1.662	9.163	2.612	9.160	2.429	6.029	2.932	6.027	2.620	3.028	3.012	3.032	2.977
16.231	.918	16.245	.803	12.975	1.673	12.959	1.523	9.675	2.569	9.673	2.500	6.225	2.926	6.227	2.620	3.128	3.022	3.200	3.003
17.165	.828	17.164	.810	13.699	1.531	13.626	1.517	10.128	2.512	10.127	2.507	6.766	2.917	6.766	2.916	3.268	3.033	3.368	3.029
Leading-edge radius: 0.077				Leading-edge radius: 0.065				Leading-edge radius: 0.054				Leading-edge radius: 0.042				Leading-edge radius: 0.031			

¹Locations of stations are measured in inches from plane of symmetry.



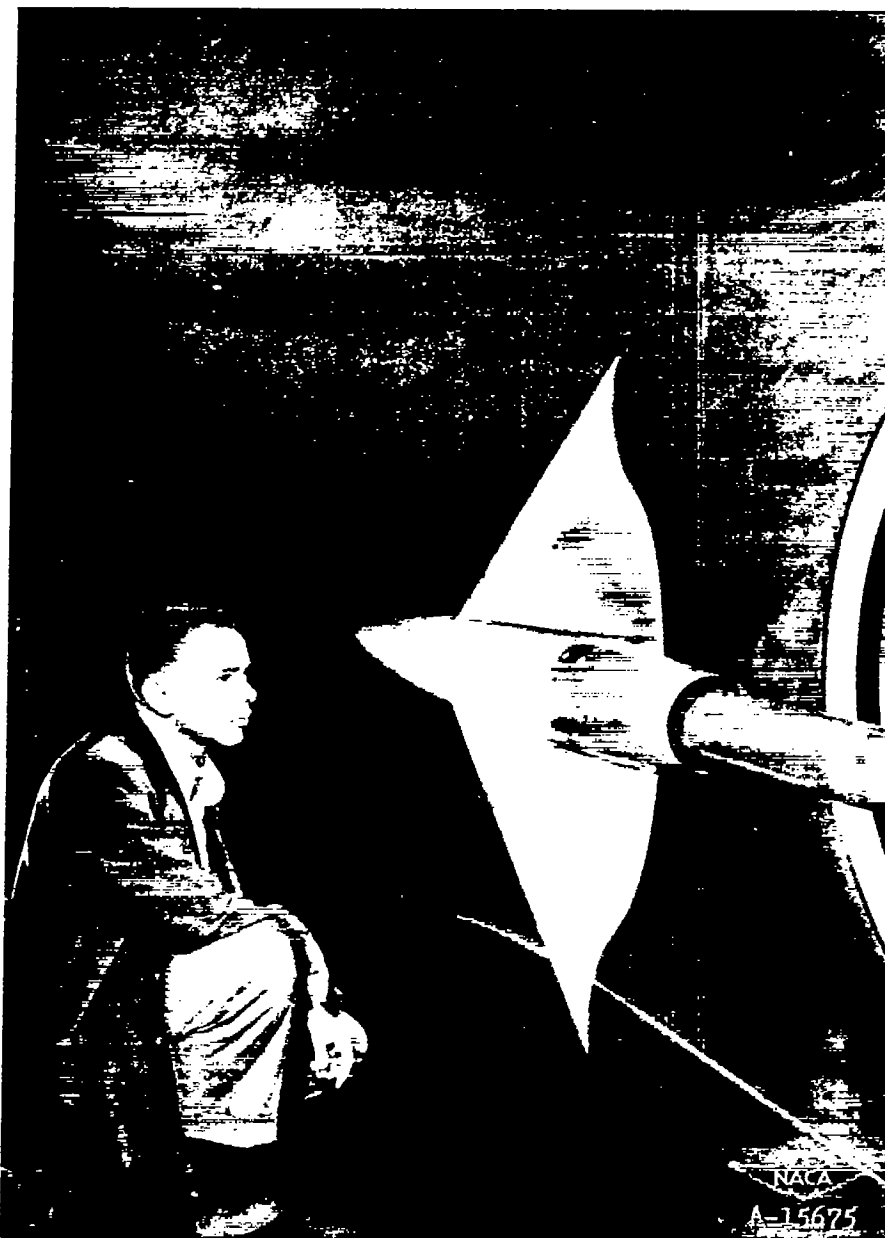


Figure 1.— Model in the Ames 6— by 6—foot supersonic wind tunnel.

Equation of fuselage radii:

$$\frac{r}{r_0} = \left[1 - \left(1 - \frac{2x}{l} \right)^2 \right]^{3/4}$$

All dimensions shown in inches
unless otherwise noted

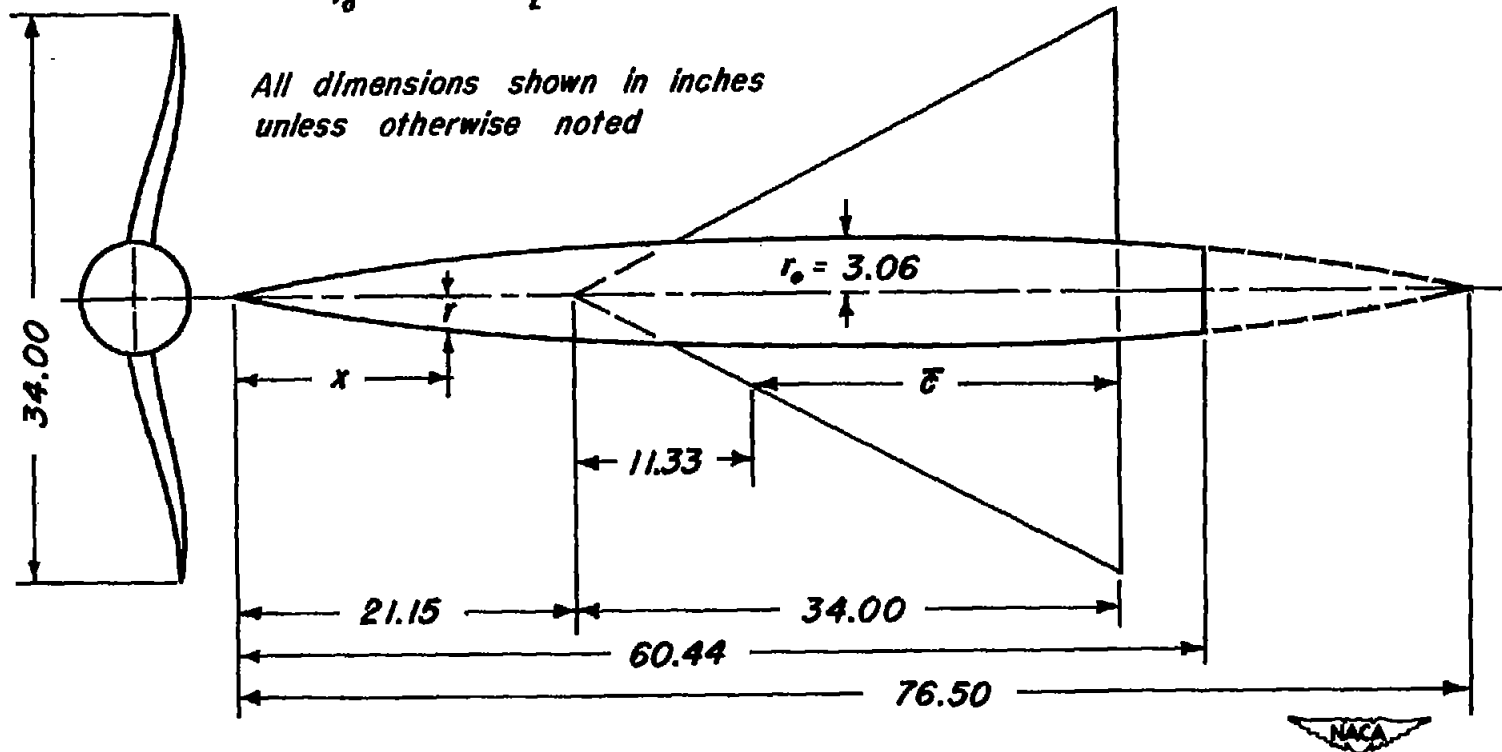
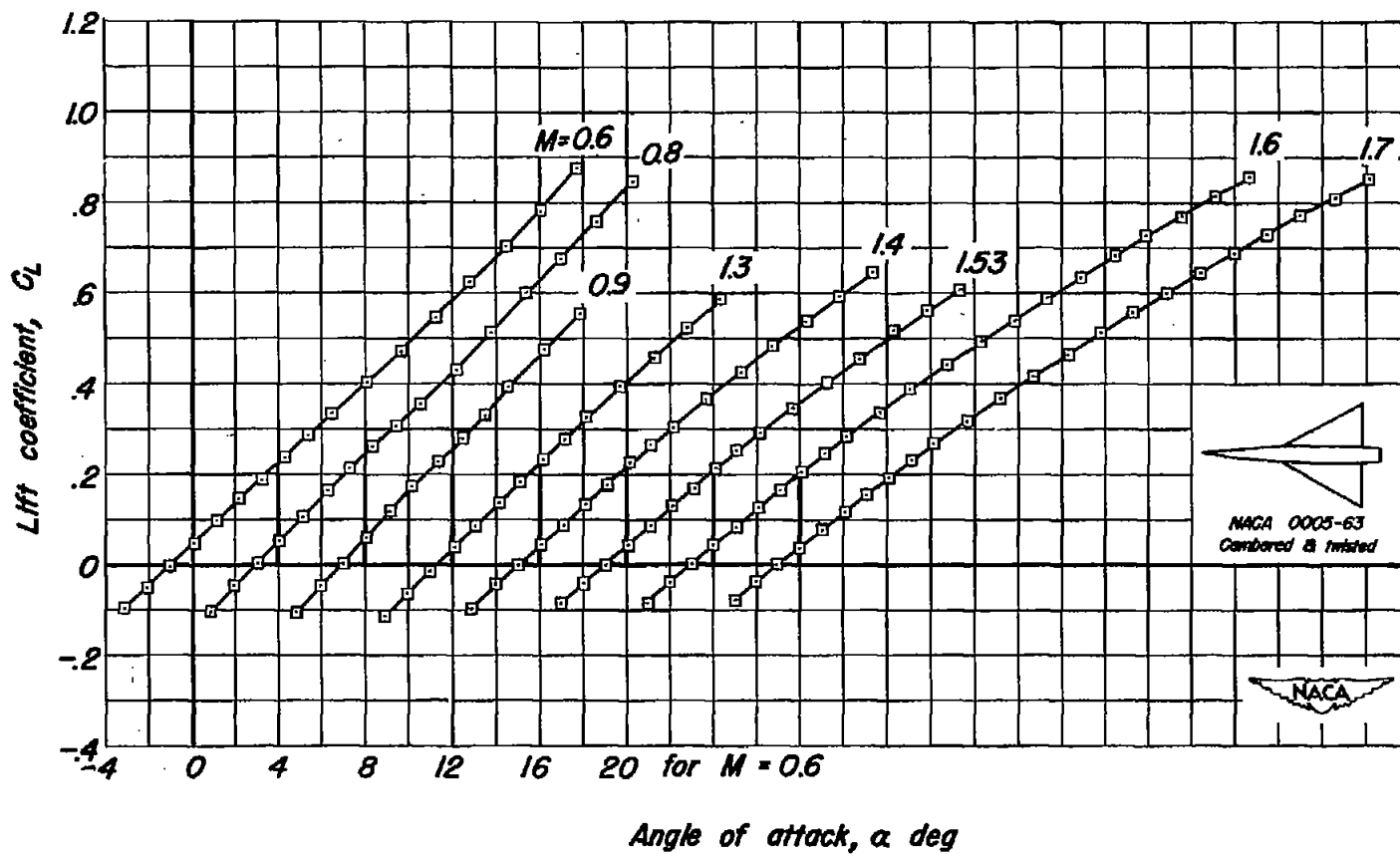
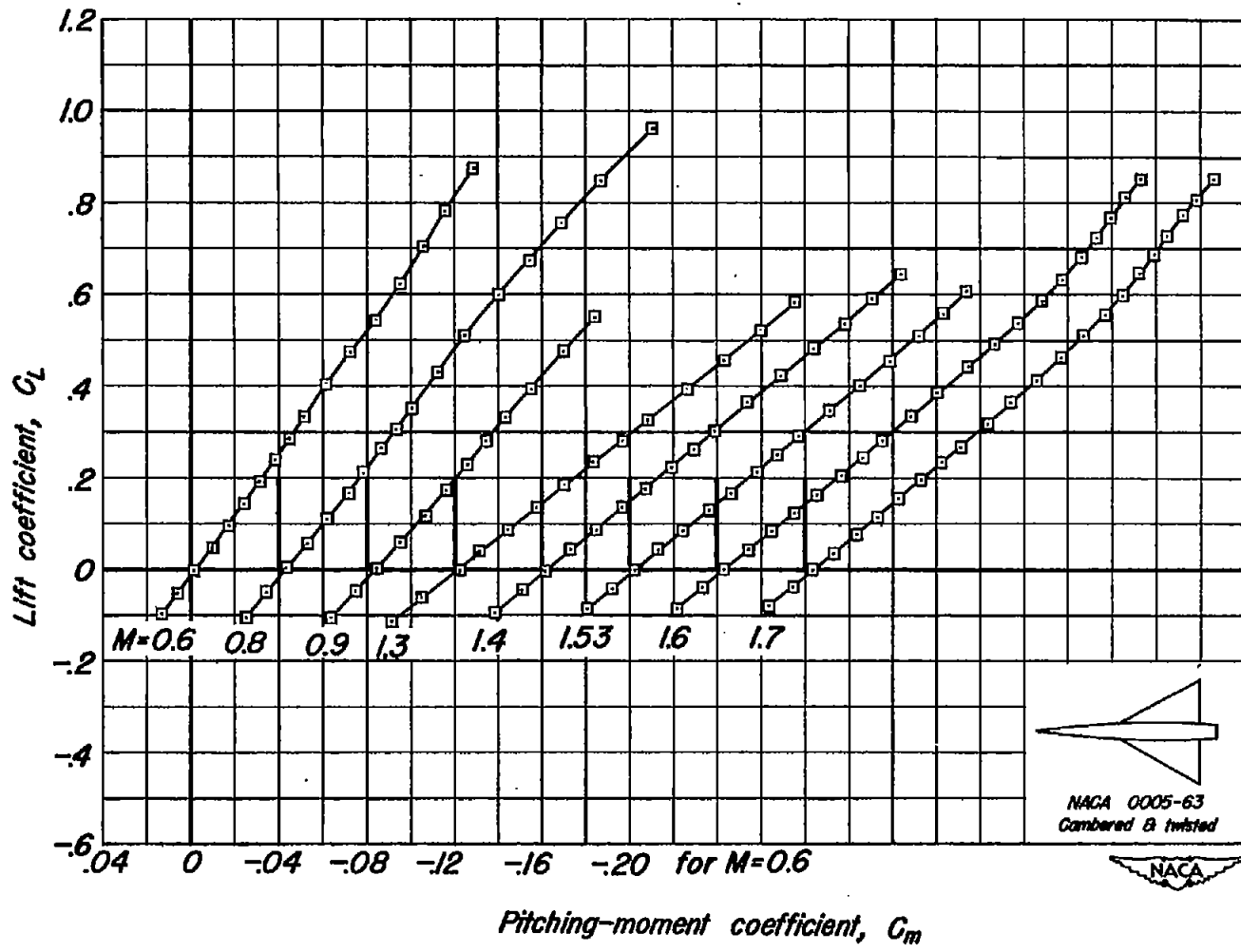


Figure 2. — Plan and front views of the model.



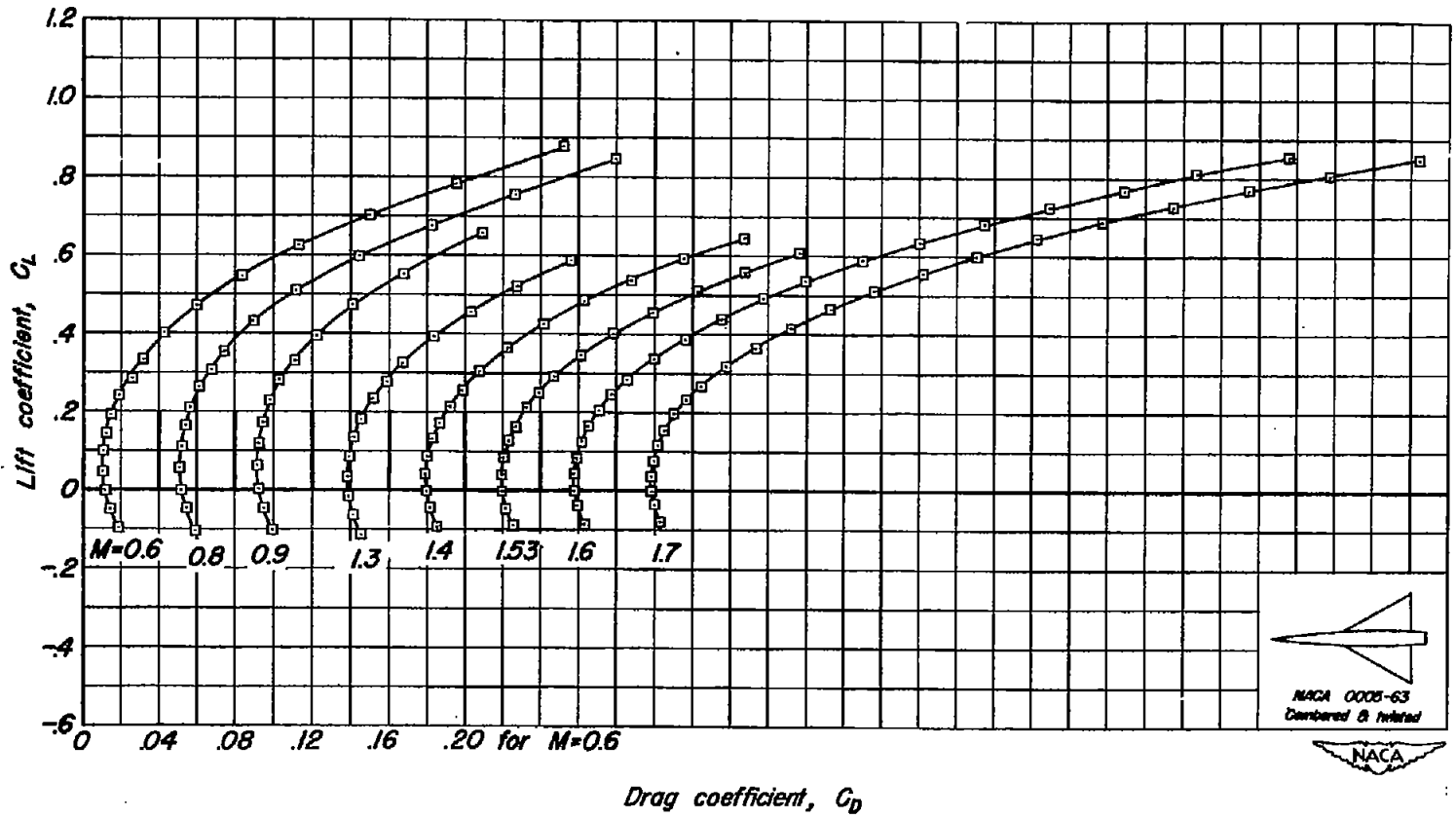
(a) C_L vs α

Figure 3.— The variation of the aerodynamic characteristics with lift coefficient at various Mach numbers. Reynolds number, 3.0 million.



(b) C_L vs C_m

Figure 3.- Continued.



Drag coefficient, C_D

(c) C_L vs C_D

Figure 3.— Continued.

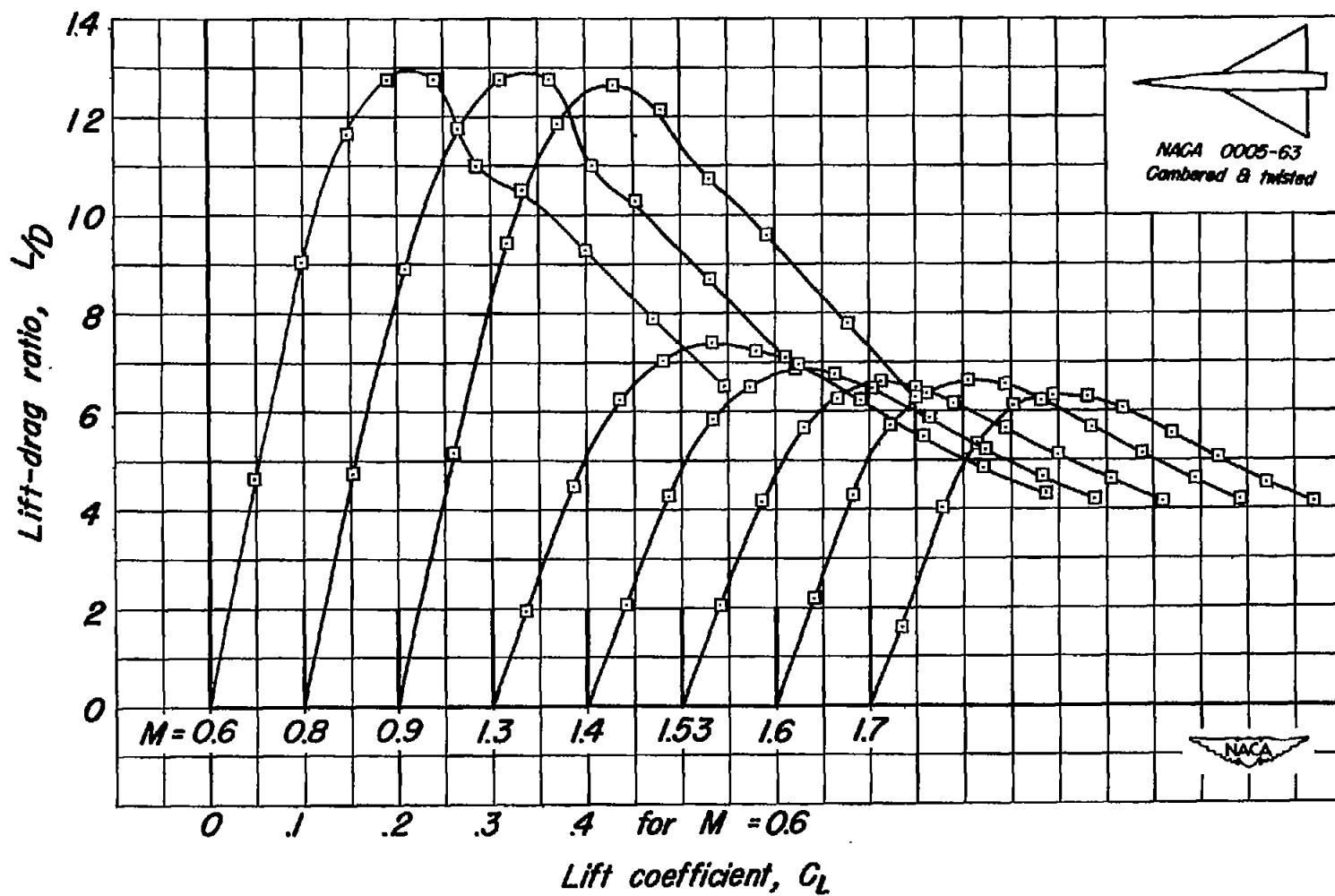


Figure 3.— Concluded.

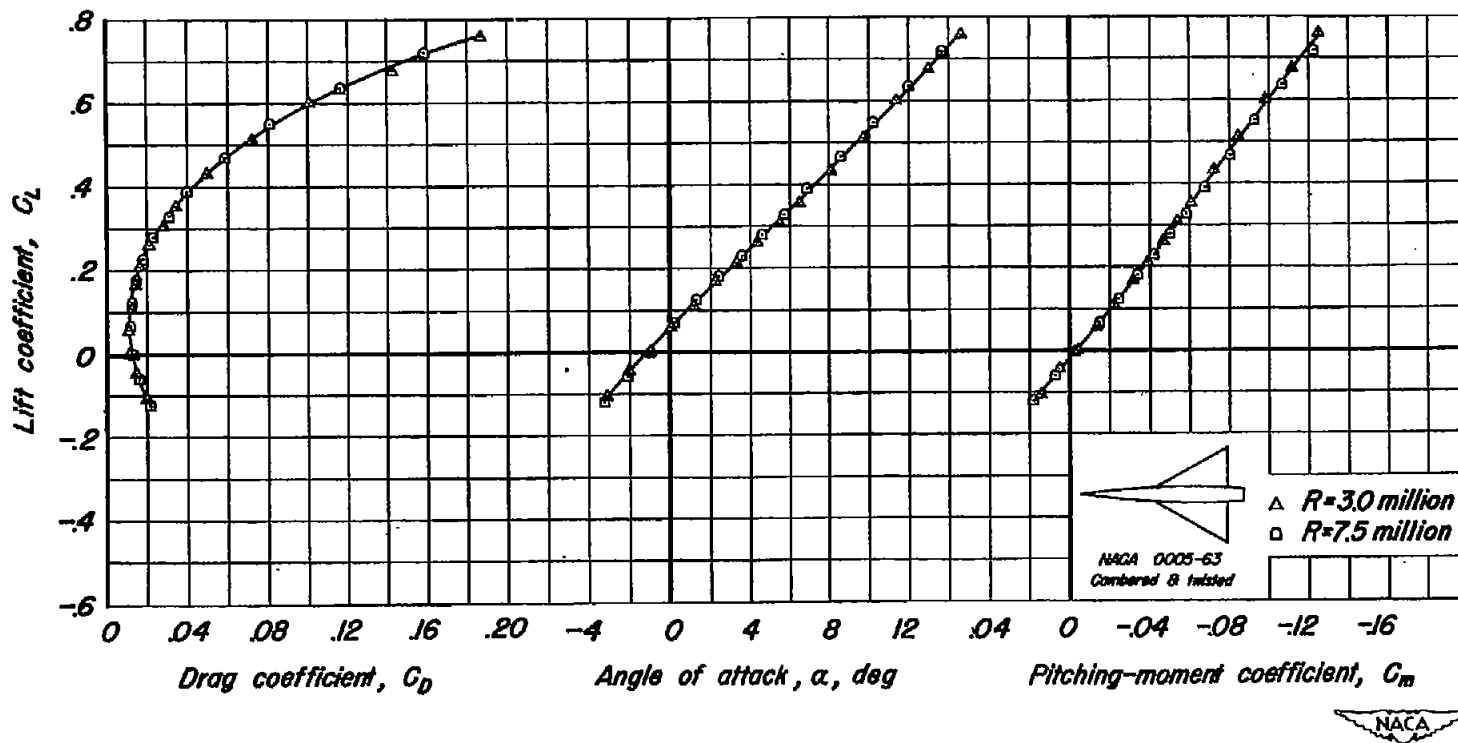
(a) $M=0.8$

Figure 4.—The variation of the aerodynamic characteristics with lift coefficient at various Reynolds numbers.

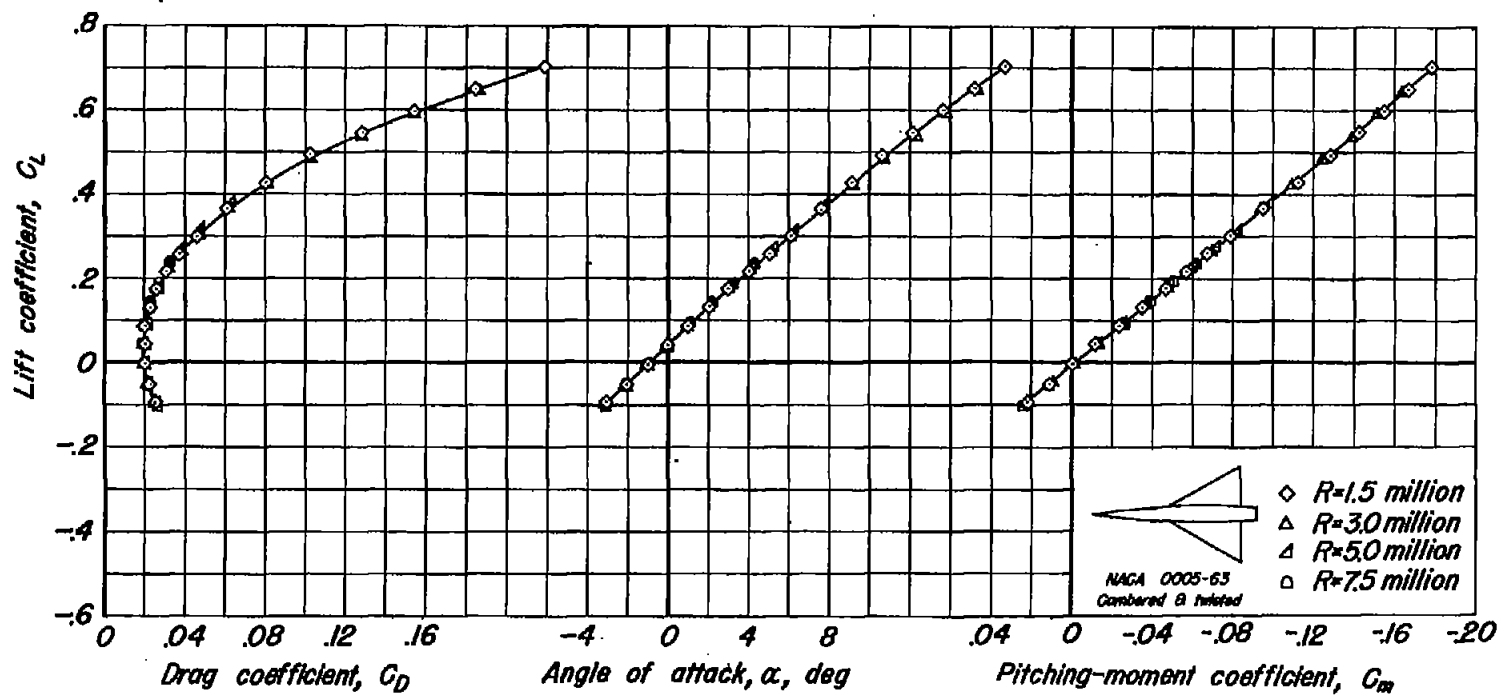
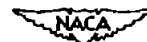
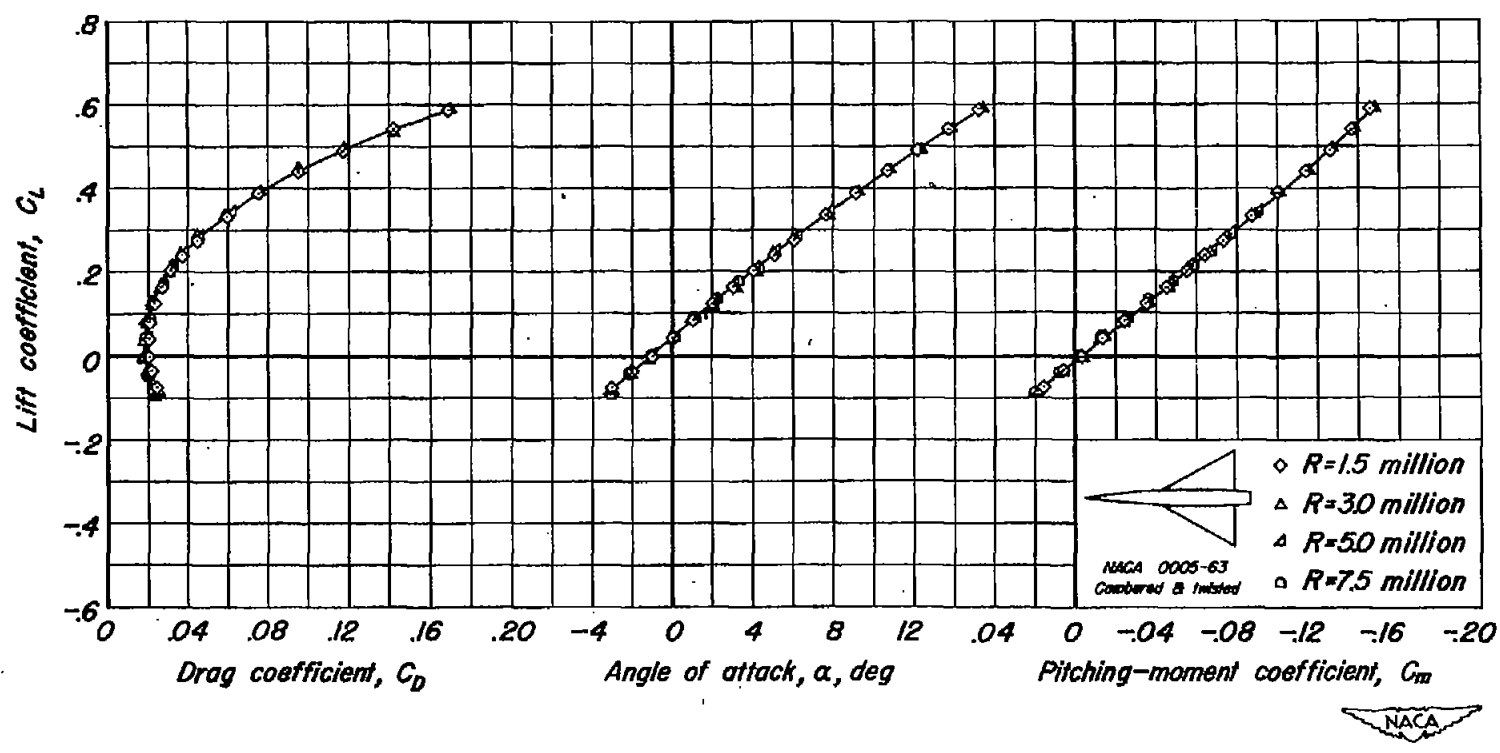
(b) $M=1.4$

Figure 4.— Continued.





(c) $M=1.6$

Figure 4.— Concluded.

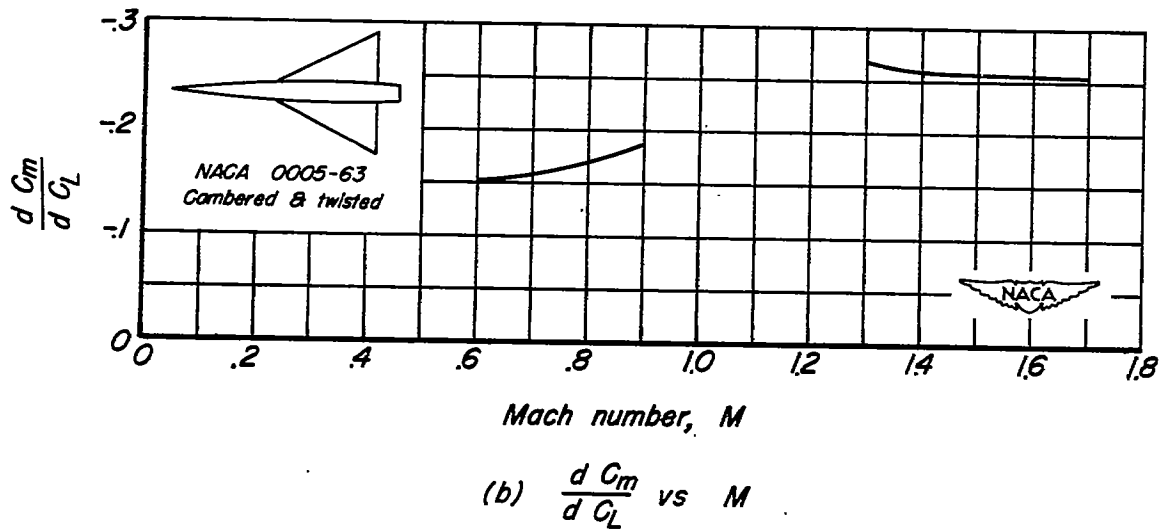
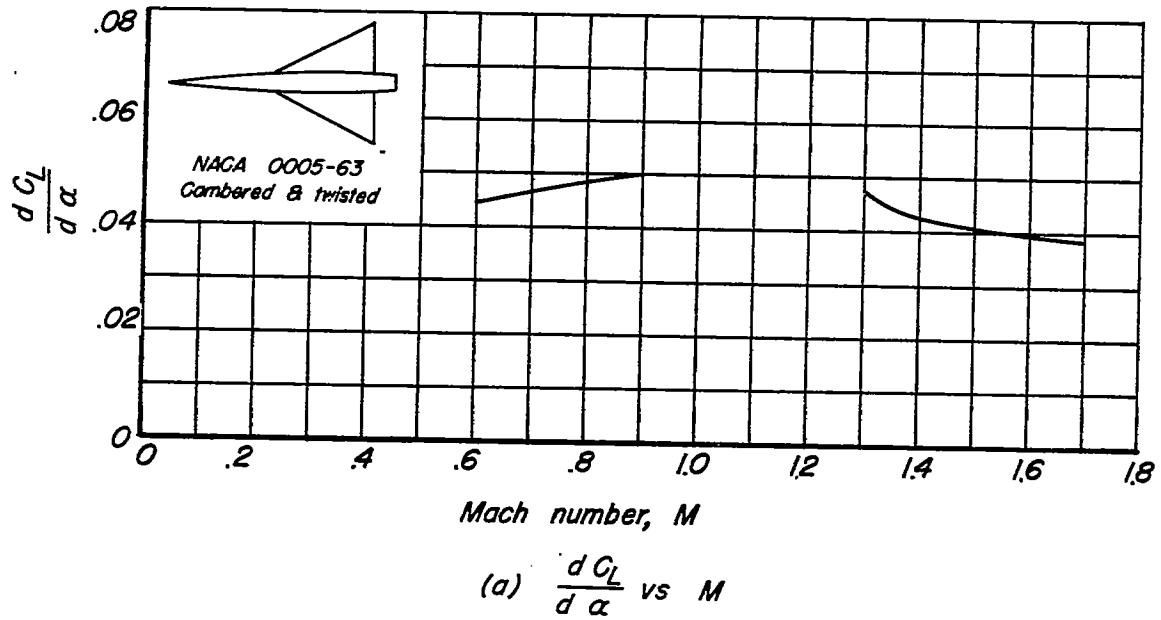


Figure 5.— Summary of aerodynamic characteristics as a function of Mach number. Reynolds number, 3.0 million.

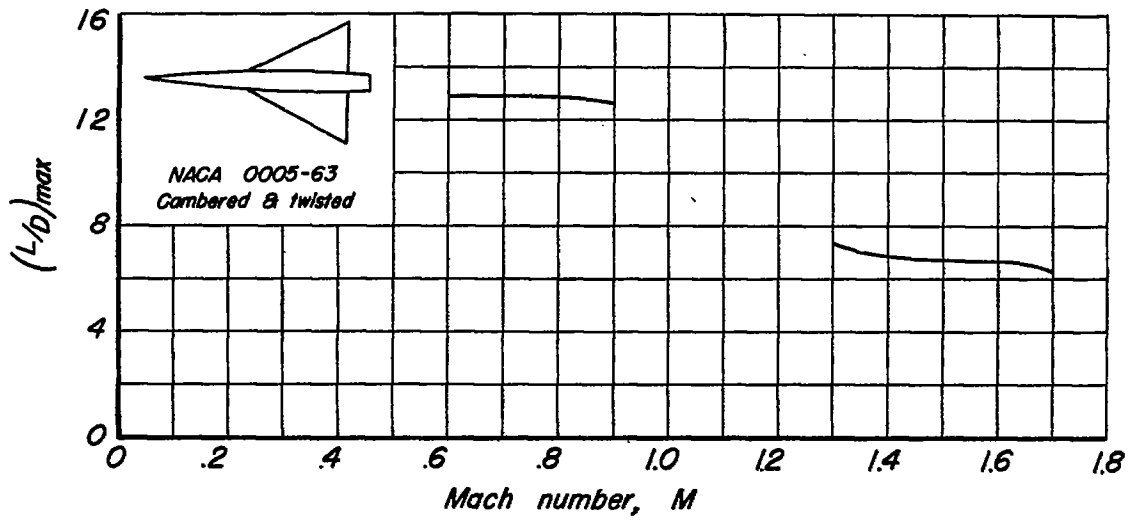
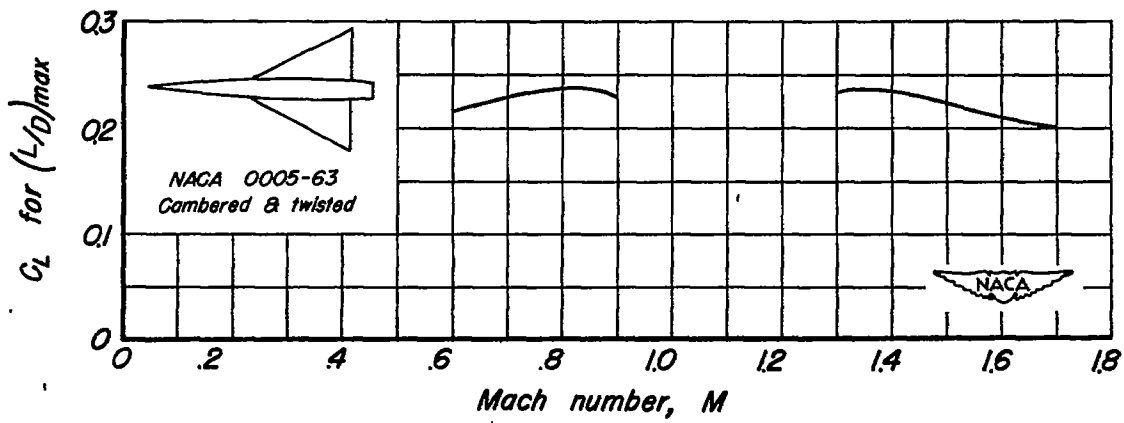
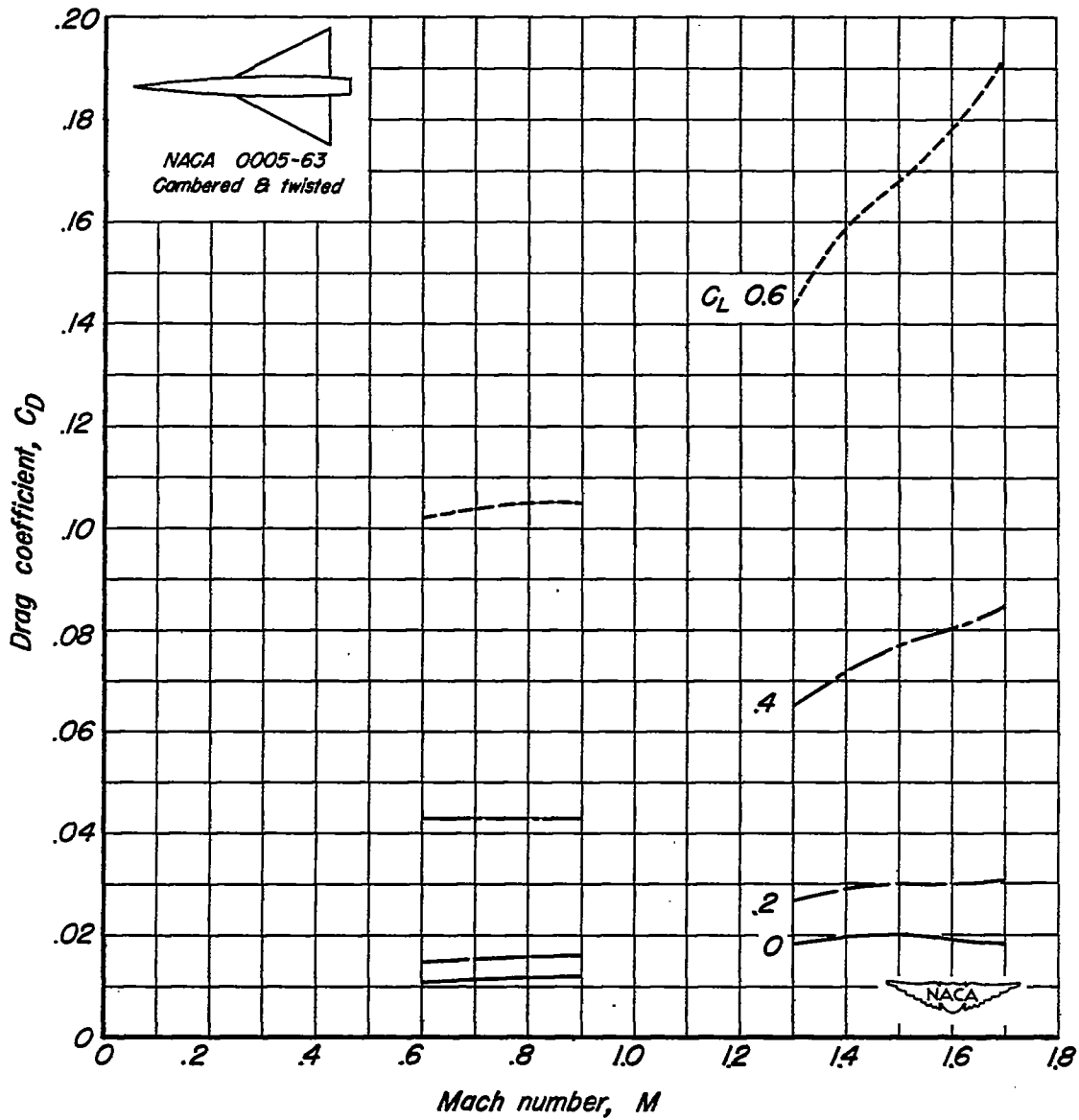
(c) $(L/D)_{max}$ vs M(d) C_L for $(L/D)_{max}$ vs M

Figure 5.— Continued.



(e) C_D vs M

Figure 5.— Concluded.